MIMO Capacity of Wireless Mesh Networks

Sebastian Max, Bernhard Walke
Communication Networks (ComNets) Research Group
Faculty 6, RWTH Aachen University, 52074 Aachen, Germany
Email:{smx|walke}@comnets.rwth-aachen.de

***Abstract*—A Wireless Mesh Network (WMN) serves to extend the wireless coverage of an Internet gateway by means of Mesh Stations (MSTAs) that transparently forward data between Stations (STAs) and the gateway. This concept reduces deployment costs by exchanging the multiple gateways, required to cover a larger area with wireless Internet access, by a wireless backbone. Unfortunately, this also reduces capacity, owing to multiple transmissions of the same data packet on its multi-hop route. Hence, different mechanisms to increase the capacity of WMNs are investigated.**

Multiple Input/Multiple Output (MIMO) is a technique that is able to increase the capacity of a single link in the same bandwidth and transmission power: Both the transmitter and the receiver is configured with multiple antennas. If multiple streams are transmitted in a rich scattering environment, these streams can be separated and decoded by the receiver successfully.

However, it is unclear how this single-link capacity increase translates into a system capacity increase in a WMN. In this paper, we will combine a realistic MIMO model with a capacity calculation framework to show the combined effect of the two technologies. The results show that although not the full link capacity increase of MIMO can be exploited, especially WMNs benefit from the MIMO gain.

***Keywords*–Wireless Networks, Capacity, Multiple-Input/Multiple-Output (MIMO), Mesh**

I. Introduction

In the last years, two parallel research areas have produced fundamental innovations for wireless data networks: First, the exploitation of multipath propagation by multiple transmit and receive antennas to increase the link capacity using the same bandwidth. Second, the upcoming of Mobile Ad-Hoc Networks (MANETs) where data is forwarded by intermediate nodes on dynamic, self-configured paths to extend the range of a single wireless link.

In both areas the innovations have successfully found their way into standards and products: Multi-antenna technology, also known as Multiple Input/Multiple Output (MIMO), is for example a crucial part of the latest amendment of IEEE 802.11, "n" [2], to reach the maximum gross throughput of 600 Mb/s (using, among other techniques, 4 transmit and receive antennas). And while MANETs are not deployed themselves, the results from the research of wireless path selection protocols are now standardised and implemented in Wireless Mesh Networks (WMNs), e. g., in [3]: In contrast to MANETs, data forwarding is restricted to special Mesh Stationss (MSTAs), implementing the *mesh facility*. This facility enables forwarding of frames between MSTAs so that for example the limited radio coverage of a Internet-connected MSTA (named *mesh gate* according to [3]) is extended without new wires. Throughout the paper, it is assumed that MSTAs also provide the Access Point (AP) facility for association and management of mobile Stations (STAs). From their viewpoint, the coverage extension via relaying is completely transparent.

The two research areas are parallel two each other because they are applied to different layers of the OSI/ISO protocol stack: MIMO is a technology applied mostly by the Physical Layer (PHY), plus some intelligence in the Medium Access Control (MAC) required for the advanced Rate Adaptation (RA) that now incorporates, next to the selection of the Modulation- and Coding Scheme (MCS), the number of streams to be transmitted. In contrast, the ability to forward data transparently for the application over multiple hops is at the heart of the Network Layer (NL), with probably some improvements in the MAC to measure the wireless link quality or to schedule multi-hop transmissions. Hence, due to the characteristics of the OSI/ISO protocol stack model, it is straightforward to combine the advances of the PHY to those of the NL; as a matter of fact, the two technologies should be transparent to each other.

While this statement is true from a qualitative perspective, its quantitative implications are unknown: In theory, MIMO provides a link capacity improvement which scales linearly with the number of transmit/receive antennas. Of course, this capacity increase would be advantageous especially for the wireless backbone between the MSTAs where the aggregated data of the mobile STAs is transported. However, it is not clear how much of the link capacity increase of MIMO remains to the system capacity of the WMN.

The scope of this paper is to estimate the improvements of MIMO in a WMN. It is structured as follows: After reviewing the related work on capacity estimation of wireless networks in Section II, Section III details the applied system model. At first, this system model is

applied to a single Basic Service Set (BSS), consisting of multiple STAs and a single AP, in Section IV to estimate the upper bound BSS capacity for a WMN. Then, Section V introduces the capacity calculation method for WMNs. This calculation method is applied in Section VI to evaluate the effect of different MIMO configurations. Finally, the paper concludes with Section VII.

II. Related Work

Capacity calculation of wireless communication networks is a popular research topic. Two major trends have evolved:

1) To determine the capacity bound of a random network with certain properties, where the capacity is considered to be a random variable and asymptotic properties are calculated, and
2) To compute the capacity of a given, arbitrary network using graph-theory based algorithms.

Besides these trends, work has been published that considers a given network for calculating its capacity from the shortest possible schedule by means of Linear Programming.

1) Analytical Bounds: In their seminal paper Gupta and Kumar [4] explored the limitations of multi-hop radio networks with random source-destination traffic relationships by computing the achievable throughput for a random network obtained under optimal conditions to be $\Theta\left(W/\sqrt{n}\right)$, where n is the number of nodes and W the radio bandwidth.

Gupta and Kumar conclude that efforts should be targeted to small networks, where nodes communicate with near neighbours only.

Several researchers have considered to extend this basic model, e. g., by incorporating different network structures [5] or mobility of nodes [6]. Due to the same approach chosen, these papers have in common that they derive asymptotic scaling laws to describe the capacity bounds for the considered random network. Application of these results to any real WMN instance with a given topology appears not to be possible.

2) Graph-based capacity calculation: The mentioned disadvantage is avoided when concentrating on the calculation of capacity bounds in a given network instance. In [7] and [8] this is done by translating the properties of the wireless medium (shadowing, interference, receive probability) into two graphs: The connectivity graph $G = (V_G, E_G)$ and the conflict graph $C = (V_C = E_G, E_C)$. While in G each vertex represents a node and an edge represents a link between two nodes, C represents links that cannot transmit simultaneously. The capacity of the network is computed then using methods from graph-theory.

Since computation of the capacity bounds of a given wireless network is NP-complete even under simple assumptions [9], approximation algorithms must be used.

For real-world wireless networks where link adaptation is state of the art, the problem is even aggravated: A node may choose among alternate MCSs to be used for a transmission. If a high-rate, but interference susceptible MCS is chosen, the link should be operated under low interference only, in contrast to a more robust, low-rate MCS that may function well under high interference. Hence, it is impossible to generate the conflict graph C without assigning to each link a single MCS in advance. Therefore, most papers on capacity calculation restrict the link model to one MCS only, thereby ignoring an important characteristic of current wireless standards.

3) Linear Programming-based capacity calculation: Algorithms published for calculating the system capacity of a given network taking different MCSs into account all use a model similar to the one introduced in [10]: Alternate assignments of MCSs are compared by computing the set of achievable data rate combinations between all source-destination pairs in the network. *Basic Rates* are introduced as a key element, describing a set of links active at a given time. The challenge is to find the schedule of all feasible basic rates that minimises the schedule's duration. A capacity bound can be derived from the duration of the shortest schedule and the amount of carried traffic. Consistent with [9], the number of basic rates and thus the algorithm runtime complexity grows exponentially, rendering it useless for networks with more than 30 nodes.

Reference [11] proves the computation of the shortest schedule to be NP-complete and extends the work of [10] by a column-based approach to solve the Mixed-Integer Programming (MIP)-formulation of the optimisation problem. Although this method makes use of modern branch-and-price methods to solve the MIP, large networks with 40 and more nodes cannot be solved exactly. Instead it is proposed to stop the branching process using a heuristic.

4) Previous Publications by the Authors: The concept of linear programming-based capacity calculation is picked up by the authors in [12], where the heuristics Selective Growth (SG) and Early Cut (EC) to control the number of network states are introduced and applied to WMNs first. A more detailed analysis and the additional heuristic Selective Growth/Delete (SG/Del) is provided by [13]. These extensions to the linear programming method are crucial to compute the capacity of large-scale scenarios with 100 and more nodes.

The improved calculation methods have been applied by the authors to calculate the capacity of WMNs under different conditions: [14] considers hybrid wireless/wired mesh networks, [15] uses Ultra Wideband

(UWB) as transmission technology and [1] shows the effect of transmit power control on the capacity. Throughout the publications, the capacity calculation method has proven to be a versatile tool to estimate the effect of a PHY technology to the system capacity.

III. System Model

The system model is especially concerned with the characteristics of a wireless network, i. e., the the wireless channel and the performance capability of the PHY to transmit information using the wireless channel. In compliance with the topic of the paper. According to the topic of the paper, special treadment is given to model MIMO transmissions.

A. Wireless Channel Model

The wireless channel determines the received signal strength of a transmission from node N_i to N_j, positioned at p_i and p_j, respectively. Typically, a wireless channel model is of the form

$$\mathrm{P}\left(N_i, N_j\right)[\mathrm{dBm}] = \mathrm{P}_i + g_i + g_j \tag{1}$$
$$- \mathrm{pl}(p_i, p_j) - \mathrm{s}(p_i, p_j) \tag{2}$$

where

- P_i is the transmission power of node N_i;
- g_i and g_j are optional transmit and receive antenna gains;
- $\mathrm{pl}(p_i, p_j)$ is the pathloss function that models the attenuation of the radio wave due to the distance between N_i and N_j;
- $\mathrm{s}(p_i, p_j)$ is a shadowing fading component having log-normal distribution.

The system performance highly depends on the characteristics of this model, i. e., the parameterisation of $\mathrm{pl}(p_i, p_j)$ and $\mathrm{s}(p_i, p_j)$. Therefore, it is crucial that the selection is based on extensive real-world measurements campaigns. Furthermore, the usage of a standardised model allows direct comparison with results from the literature that use the same assumptions.

Based on these considerations and the typical application scenario of a WMN, we select the Urban Micro (UMi) channel model described in [16], which is designed to evaluate radio interface technologies in the IMT-Advanced process. This model provides pathloss functions for Line Of Sight (LOS), Non Line Of Sight (NLOS) and Outdoor-to-Indoor (OtoI) links as well as a description of a random process with correlated log-normal distribution for the shadowing fading.

B. Physical Layer Model

The Physical Layer (PHY) model decides under which conditions a packet transmission is successful, i. e., the packet is decoded error-free at the receiver.

In our model, the success probability depends on two factors:

1) How much noise from the background and other active transmissions interferes with the signal and
2) which MCS is selected at the transmitter.

Throughout the paper we will assume IEEE 802.11n-2009 [2], as the physical layer standard. Adaptation of the methodology to other wireless transmission technologies based on Orthogonal Frequency Division Multiplexing (OFDM) is possible by adapting the calculations to different MCS; however, this is not in the scope of this paper.

As in [2], the MCS does not only comprise the modulation and the channel coding, but in addition the number of spatial streams n_{ss}. Hence, the MCS comprises all information that determines the number of data bits per OFDM symbol.

1) SINR: Signal degradation at the receiver is caused by two factors: First, the thermal- and receiver noise; second, interference from other active transmissions.

The power of thermal noise (dBm) is given by $N_{th} = -174 + 10\log_{10}(\Delta_f)$, where Δ_f is the bandwidth in Hz ; the receiver noise N_{rx} is an additional degradation caused by components in the RF signal chain and assumed to be 5 dB.

Let now denote N_j the current receiver, trying to decode a signal from N_j, starting at time t_0 and ending at t_1. Furthermore, let $\mathbb{I} = \{k : k \neq i, k \neq j\}$ be the set of active transmitters of all other overlapping transmissions, having start time $t_{k,0}$ and end time $t_{k,1}$.

Then the interference $I_{i,j,\mathbb{I}}$ at N_j for the transmission from N_i is computed in mW as

$$I_{i\to j,\mathbb{I}} = \sum_{k\in\mathbb{I}_{i\to j}} \frac{\min\left(t_1, t_{k,1}\right) - \max\left(t_0, t_{k,0}\right)}{t_1 - t_0} \cdot \mathrm{P}\left(N_k, N_j\right). \tag{3}$$

This calculation averages each interfering signal over the transmission time; hence, the effect of strong but short interference peaks are underestimated. This simplification is tolerable when using the capacity calculation methods described below, as interference will be aligned optimally.

The final quality of the received signal is measured by the Signal to Interference plus Noise Ratio (SINR):

$$\mathrm{SINR}_{i\to j} = \frac{\mathrm{P}\left(N_i, N_j\right)[\mathrm{mW}]}{I_{i\to j,\mathbb{I}}[\mathrm{mW}] + \left(N_{th} + N_{rx}\right)[\mathrm{mW}]}. \tag{4}$$

2) Packet Error Rate: The resulting Packet Error Rate (PER) of a received frame, which corresponds to the probability of a data burst with faulty Cyclic Redundancy Check (CRC), depends on three parameters: the MCS which is selected by the transmitter, the frame size, and the SINR measured at the receiver.

Based on the SINR and the modulation scheme, the pre-decoder Bit Error Rate (BER) can be derived analytically for the modulation schemes defined in IEEE 802.11 as shown in [17].

IEEE 802.11 specifies two channel coding schemes, namely Binary Convolutional Code (BCC) and Low-Density Parity-check Code (LDPC). In this paper, we restrict ourselves to the BCC scheme. Hence, the results from [18] can be applied, allowing for estimating an upper bound for the PER dependent on the SINR and the packet length.

3) Link Throughput: For an error-free link, the link gross throughput using MCS m is given by the number of data bits per symbol, n^m_{DBPS}, divided by the duration of one symbol:

$$T^m = n^m_{DBPS}/t_{symbol} \tag{5}$$

C. Modelling MIMO Links

Coarse classification distinguishes two types of MIMO techniques (both part of IEEE 801.11n-2009) based on the propagation channel properties, i. e., on the structure of the spatial correlation matrix at the antenna array. In the case of high correlation of the transmitted signal beamforming can be applied, whereas in the case of low correlation diversity and multiplexing approaches apply [19]. The focus of this work is MIMO methods in the later sense, namely Spatial Multiplexing (MUX) and Spatial Diversity (DIV) schemes.

In MUX schemes, $n_{ss} > 1$ streams are transmitted simultaneously, each one using one dedicated antenna of the transmitter. In a rich scattering environment the signal of the combined streams takes different paths with none or low correlation. Hence, different signals arrive at the multiple receive antennas which can be processed to gain the different streams. Obviously, the number of data streams is limited by the number of transmit antennas, n_{tx}. Furthermore, the receiver must contain at least as many receive antennas, n_{rx}, as streams. Consequently, a MUX scheme increases the data rate at most by $\min(n_{tx}, n_{rx})$.

DIV schemes, in contrast, exploit the diversity of the multiple receptions of the same signal: The receiver with multiple antennas has multiple copies of the transmitted signal, each distorted by a different channel function. Thus, appropriate signal processing algorithms can increase the SINR of the signal by combining the different streams.

In the schemes combining MUX and DIV, more than one transmit antenna is active, but the receiver, as in DIV schemes, has more antennas than the number of spatial streams transmitted. To describe a link with n_{tx} transmit and n_{rx} receive antennas, the common notion "$n_{tx} \times n_{rx}$" will be used. If not mentioned otherwise, we will assume that either $n_{ss} = n_{tx}$ or that the transmitter deactivates $n_{tx} - n_{ss}$ antennas to transmit $n_{ss} < n_{tx}$ streams.

A detailed introduction to the history, benefits and problems of MIMO systems can be found in [20].

1) Signal Model: A $n_{tx} \times n_{rx}$ MIMO system is represented by Equation 6 where it is assumed that the total transmit power is equally divided over the n_{tx} transmit antennas:

$$\mathbf{y} = \sqrt{\frac{E_S}{n_{tx}}}\mathbf{H}\mathbf{s} + \mathbf{n}; \tag{6}$$

$\mathbf{s} \in \mathbb{C}^{n_{tx} \times 1}$ is the transmitted signal vector whose jth component represents the signal transmitted by the jth antenna. Similarly, the received signal and received noise are represented by $n_{rx} \times 1$ vectors, $\mathbf{y}$ and $\mathbf{n}$, respectively, where y_j and n_i represent the signal and noise received at the ith antenna. E_S denotes the average signal energy during the transmission. Finally, $\mathbf{H} \in \mathbb{C}^{n_{rx} \times n_{tx}}$ is the matrix representing the $n_{rx} \cdot n_{tx}$ channels between the n_{tx} transmit and n_{rx} receive antennas.

If $n_{ss} = n_{tx} = n_{rx}$ and $\mathbf{H}$ has full rank, i. e., $\mathbf{H}^{-1}$ exists, the Zero-Forcing (ZF)-receiver can extract $\mathbf{s}$ as follows:

$$\hat{\mathbf{s}} = \left(\sqrt{\frac{E_S}{n_{tx}}} \cdot \mathbf{H}\right)^{-1} \mathbf{y}. \tag{7}$$

This equation can be generalised for $n_{tx} \neq n_{rx}$ by using the Moore-Penrose pseudo-inverse matrix $\mathbf{H}^\dagger = \mathbf{H}^* / (\mathbf{H}^*\mathbf{H})$ instead of $\mathbf{H}^{-1}$, where $\mathbf{H}^*$ is the conjugate transpose of $\mathbf{H}$.

Under ideal circumstances, one may increase the data rate of the system by merely adding transmit and receiver antennas. Under realistic conditions, there is non-neglectable correlation between the transmit and receive antennas: In the extreme case, the channel $\mathbf{H}$ is equal to $\left(\begin{smallmatrix} 1 & 1 \\ 1 & 1 \end{smallmatrix}\right)$, which resembles a completely correlated channel. In this case, the matrix is singular and cannot be inverted by the receiver; hence, the reception fails, independently of the SINR.

In practice, the MIMO channel does not fall completely in either of the theoretical cases described. The antenna correlation and the matrix rank are influenced by many different parameters, as the antenna spacing, antenna height, the presence and position of local and remote scatterer, the degree of LOS and more.

Using a widely accepted channel model, the MIMO channel with correlated antennas can be described by the matrix product

$$\mathbf{H} = {\mathbf{R_{rx}}}^{1/2}\mathbf{H_0}{\mathbf{R_{tx}}}^{1/2}, \tag{8}$$

where $\mathbf{H_0}$ represents the i. i. d. block fading complex Gaussian channel according to [21] and $\mathbf{R_{rx}}$ and $\mathbf{R_{tx}}$ are the long-term stable normalised receive and transmit correlation matrices.

Link Type	Angle Spread (rad)	
	APs	STAs
LOS	0.2766	0.9815
NLOS	0.4486	1.2075
OtoI	0.3104	1.004

TABLE I: Parameters for the UMi angle of arrival/departure spread

Under the assumption of a uniform linear array at both the transmitter and the receiver with identical unipolarised antenna elements and the antenna spacing Δ_T and Δ_R, respectively, the correlation matrices are given by [22]:

$$\mathbf{R}_{\mathbf{rx}i,j} = \rho\left((j-i)\Delta_R, \theta_R, \sigma_R\right) \tag{9}$$

$$\mathbf{R}_{\mathbf{tx}i,j} = \rho\left((j-i)\Delta_T, \theta_T, \sigma_T\right), \tag{10}$$

where

- $\rho\left(s\Delta, \theta, \sigma_\theta\right)$ defines the fading correlation between two antenna elements having distance $s\Delta$,
- θ_T and θ_R denote the mean Angle of Departure (AoD) at the transmit array and the mean Angle of Arrival (AoA) at the receive array, respectively, and
- σ_T and σ_R is the mean AoD spread and mean AoA spread, respectively.

A Gaussian angular distribution is used in [16], implying that $\theta \sim N(0, \sigma)$. With this assumption it is shown in [23] that

$$\rho\left(s\Delta, \theta, \sigma\right) \approx e^{-j2\pi s\Delta\cos(\theta)} e^{-1/2(2\pi s\Delta\sin(\theta)\sigma)^2}. \tag{11}$$

Essentially, this model results in a correlation function which is Gaussian with spread inversely proportional to the product of antenna spacing and angle spread. Consequently, large antenna spacing and/or large angle spread lead to a small correlation and vice versa. Support of this model is given by [24], which finds by simulation that correlation reaches a maximum with both antenna arrays inline, i. e., $\theta_T = \theta_R = 0$

While the mean AoA and AoD can be derived from the receiver and transmitter positions, respectively, the spread depends on the environment. The UMi model, used for the pathloss and shadowing, also defines values for these, given in Table I.

The model differentiates between nodes close to the ground (STAs), where many close scatterer and therefore a large angle spread can be expected, and higher-elevation nodes with less scatterer and a smaller angle.

2) Post-processing per-stream SINR: To integrate the impact of the MIMO channel model into the PER calculation from Section III-B2, we extend the model from [19] with the help of the results from [25], [26] to incorporate a correlated channel.

For this, we reconsider Equation 7 including the pseudo-inverse $\mathbf{H}^\dagger$: The ZF-receiver multiplies the received signal $\mathbf{y}$ with the matrix

$$\mathbf{G}_{ZF} = \sqrt{\frac{n_{tx}}{E_S}}\mathbf{H}^\dagger, \tag{12}$$

The error vector $\mathbf{e}$ of the processed symbol stream is given by $\sqrt{\frac{n_{tx}}{E_S}}\mathbf{H}^\dagger\mathbf{n}$, resulting in a noise power on the k^{th} data stream as

$$\left[\mathrm{E}(\mathbf{e}\mathbf{e}^*)\right]_{kk} = \frac{n_{tx}N_0}{E_S}\left[\mathbf{H}^\dagger\mathbf{H}^{*\dagger}\right]_{kk}, \tag{13}$$

where $[\mathbf{X}]_{kk}$ denotes the $(k,k)^{\text{th}}$ element of the matrix $\mathbf{X}$. Hence, the post-processing SINR on the k^{th} stream is

$$\mathrm{SINR}_{\text{post},k} = \frac{E_S\left[\mathrm{E}(\mathbf{s}\mathbf{s}^*)\right]_{kk}}{n_{tx}N_0\left[\mathbf{H}^\dagger\mathbf{H}^{*\dagger}\right]_{kk}} \tag{14}$$

$$= \frac{E_S}{N_0}\frac{1}{n_{tx}}\frac{1}{\left[\mathbf{H}^*\mathbf{H}\right]^{-1}_{k,k}}. \tag{15}$$

As visible in the equation, post-processing SINR on each stream is a combination of three factors:

1) The pre-processing SINR.
2) A reduction by n_{tx}, because the transmitter has to split its transmission energy among the n_{tx} streams.
3) A post-processing MIMO loss of $[\mathbf{H}^*\mathbf{H}]^{-1}_{k,k}$.

[25] proves that the post-processing MIMO gain on each stream follows a Chi-squared distribution with $2\left(n_{rx} - n_{tx} + 1\right)$ degrees of freedom. From this fact, it is derived that the mean gain on each stream without transmit- and receive correlation is $10\log_{10}\left(n_{rx} - n_{tx} + 1\right)$ dB.

Furthermore, [25] shows that transmit correlation causes a degradation in effective SINR that can be described by

$$K_T = 10\log_{10}\left(\left[\mathbf{R}_{tx}^{-1}\right]_{k,k}\right) \tag{16}$$

on the kth stream.

[26] calculates the impact of the receive correlation as

$$K_R = 10\log_{10}\left(\left(\frac{\mathrm{tr}_{n_{tx}-1}(\lambda(\mathbf{R}_{\mathbf{rx}}))}{\binom{n_{rx}}{n_{tx}-1}\det(\mathbf{R}_{\mathbf{rx}})}\right)^{-1/(n_{rx}-n_{tx}+1)}\right), \tag{17}$$

with

- $\mathrm{tr}_l()$ the l^{th} elementary symmetric function defined as

$$\mathrm{tr}_l(\mathbf{X}) = \sum_{\{\underline{\alpha}\}}\prod_{i=1}^{l}\lambda_{x,\alpha_i} \tag{18}$$

for a positive-definite $\mathbf{X} \in \mathbb{C}^{n\times n}$, where the sum is over all ordered sequences $\underline{\alpha} = \{\alpha_1, \ldots, \alpha_l\} \subseteq \{1, \ldots, n\}$ and $\lambda_{x,i}$ denotes the i^{th} eigenvalue of $\mathbf{X}$.

- $\lambda()$ the diagonal matrix containing the eigenvalues of the matrix argument.

To visualise the impact of the antenna correlation on the post-processing SINR, the exemplary scenario in Figure 1a is used: A receiving node is positioned in a half-circle around a transmitting node; the orientation of the node remains constant, i. e., with an angle $\alpha_{rx} = 0$ to the x-axis. With different positions, the AoD and AoA varies and so do the correlation matrices. Assuming a pre-processing SINR of 30 dB, antenna spacing of 0.5 wave-lengths and angle spreads as given in Table I (LOS), the mean post-processing SINR is given by Figure 1b. As expected, a 1×1 configuration is independent of the receiver position. All other configurations result in a post-processing SINR decrease so that the 30 dBm is not reached any more; the upper bound is given by a system without correlation, i. e., $K_T = K_R = 0$. Correlation is high if the antennas face each other or if they are parallel.

3) MIMO Link Throughput: With the help of the presented MIMO model it is now possible to compute, for given node's positions and pre-processing SINR the post-processing SINR per stream and thus the per-stream BER and PER.

As in Section III-B3, a relation SINR vs. gross throughput can be derived if AoD and AoA are given. Figure 2 omits for more clarity the different MCS but shows only the enclosing hull that can be achieved with a given MIMO antenna configuration and two nodes that face each other with parallel antenna orientation.

The graph for the 1×1 case, starting at 5 dB and levelling off at 25 dB/65 Mb/s presents the basic case that would also be possible using the legacy IEEE 802.11-2007 (plus the new 64-QAM 5/6 MCS). Adding more antennas allows to receive the signal at lower SINR levels (using DIV) and increasing the throughput (using MUX), although the full throughput gain can only be reached at very high SINR, i. e., above 33 dB for the 4×4 case.

IV. Single BSS Operation

In this chapter it is assumed that only one AP exists that uses the carrier frequency f_c. Thus, no interference from other APs or STAs that do not belong to the AP's BSS exist, the SINR is simplified to the Signal to Noise Ratio (SNR).

For wireless Internet access, this theoretical case only exists if (a) the coverage area of the AP is as large as the service area and (b) the carrier frequency is licensed to the provider. While these conditions represent only a theoretical case, performance metrics of a single BSS are important for the subsequent multi-BSS evaluation, because a single BSS is the trivial upper bound for the capacity: any deployment of multiple APs will increase the interference and/or the number of orthogonal channels and thus the used bandwidth.

The BSS capacity is given by the maximum throughput that can be achieved in a BSS under the assumption that all STAs always have data to transmit to the APs and vice versa. The capacity depends on the link capacities of the STAs in the BSS and thus on their positions. As this differs from scenario to scenario, the evaluation assumes that STAs are positioned with a uniform random distribution over the BSS area. Thus, the capacity of the BSS becomes a random variable $\mathcal{C}$ with Probability Density Function (PDF) $p_{\mathcal{C}}$. We evaluate this capacity using a Monte-Carlo approach: In one scenario, multiple STAs are dropped randomly; their capacity is calculated using the equations for the wireless channel model, the post-processing SNR and the throughput from Figure 2. This is repeated for multiple scenarios which differ by the placement of STAs and the stochastic shadowing fading.

Figure 3a shows the Cumulative Distribution Function (CDF) of BSS capacity that is generated using the Monte-Carlo method for a 1x1 to 4x4 antenna configuration. The maximum distance of a STA to the AP is chosen such that the area covered equals to the mean BSS area used in the following multi-AP evaluation, namely $0.049\,\mathrm{km}^2$.

In the 1x1 case, the expected capacity is 37.5 Mb/s, with a probability of roughly 40% that the highest MCS with 65 Mb/s is reached. With every antenna added, one more stream can be transmitted under optimal SINR condition; the maximum capacity increases accordingly up to 260 Mb/s. However, the probability that the required SINR can be reached decreases as more streams result in a lower post-processing SINR. In the end, the probability of 260 Mb/s is only 22%. Consequently, the expected capacity scales not linearly with the number of antennas, but only by a factor of 1.71, 2.26 and 2.78 for the 2x2, 3x3 and 4x4-case, respectively.

Figures 3b and 3c show the effect of the transmit and receive antenna correlation on the capacity: If both the transmit and receive angle spread is π, antenna correlation is minimal; the only factor reducing the post-SINR is the transmit power reduction to keep the total emitted power. Hence, only the minimum MIMO loss of $10 \log_{10} \left(\left(n_{rx} - n_{tx} + 1 \right) / n_{tx} \right)$ dB is incorporated. Accordingly, as visible in Figure 3b, the probability to reach the maximum capacity increases to 40% for all antenna configurations. This scales the expected capacity by 1.85, 2.69 and 3.53 for the multi-antenna cases in comparison to the 1x1 case. A further capacity increase would be possible by using highly sensitive MCSs like 256-Quadrature Amplitude Modulation (QAM) (not part of IEEE 802.11n) in the high-SINR regions.

Figure 3c shows the expected capacity if the angle

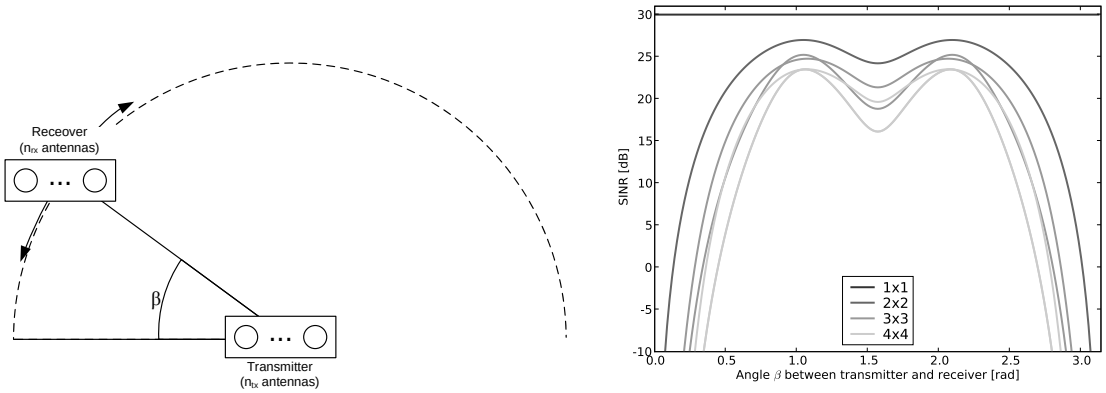

(a) Exemplary scenario with varying SINR loss due to antenna correlation.

(b) Mean post-processing SINR per stream with varying MIMO configuration.

Fig. 1: Effect of antenna correlation on the post-processing SINR.

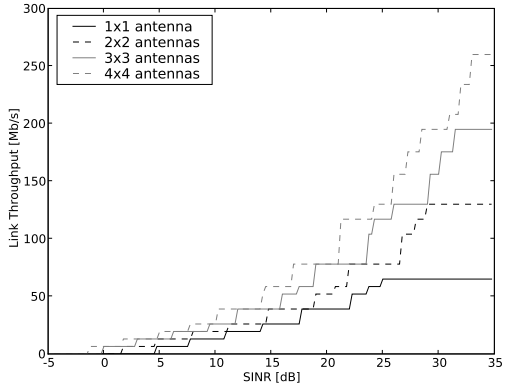

Fig. 2: Link throughput vs. SINR; assumed PSDU length is 1000 B and maximum PER 0.01.

spread is lower than in the UMi scenario: For demonstration, the angle spread from the Suburban Macro (SMa) scenario is taken (0.105 rad for the AP, 0.527 rad for STAs). As a result, the CDFs of the multi-antenna converge to the CDF of the 1x1-case. Consequently, the expected capacity increases only by 1.55, 1.81 and 2.01: Introducing complex MIMO transceivers in this scenario does not result in significant capacity gains.

V. Multi BSS Operation

The major difference between a single BSS and a WMN is the addition of interference from concurrent transmissions. In a single BSS, a concurrent transmission can only be initiated by two STAs or a AP and a STA. In the first case the AP receives two transmissions at the same time; hence, at most one signal can be decoded if transmitted using a robust MCS. In the second case, the AP is busy transmitting, there is only the chance that the downlink transmission to the STA can be received if a robust MCS is used by the AP. Both cases assume that the interference by the other STA is low, so that at least one transmission will fail and the other requires a long time due to the robust MCS. Hence, to optimise capacity, concurrent transmissions are avoided in a single BSS.

In a WMN this conclusion is not valid, because links exist that are separated from each other such that a concurrent transmission (using more robust MCS if necessary) should be preferred to a sequential operation. This is already demonstrated by the simple network shown in Figure 4, comprising four nodes and two links. It is assumed that the two links, named "1" and "2", have a maximum throughput of 30 / 22 Mb/s, if no interference is present. If both links transmit concurrently, the maximum throughput is lowered to 20 / 15 Mb/s.

If both transmitters have 1 Mb of data to transmit, it would take $1/30 + 1/22 \approx 0.079$ s until the data has reached the receivers if both links are active sequentially. Using an optimised mix of concurrent and sequential transmissions, both links transmit concurrently first; after link 1 has completed the transmission, 1-15/20 Mb are left to be transmitted at link 2, which continues at 22 Mb/s. In total, the data reaches the receivers after

$$\frac{1}{20} + \frac{1 - \frac{15}{20}}{22} \approx 0.061\,\text{s}, \tag{19}$$

thus the required duration is shortened by 22%.

Hence, the strategy deciding which links are active at what time instance is important to determine the achievable capacity of the network. In this example the calculation of the optimal distribution between sequential and concurrent transmissions is simple because only two concurrent links exist. Every link that is added to

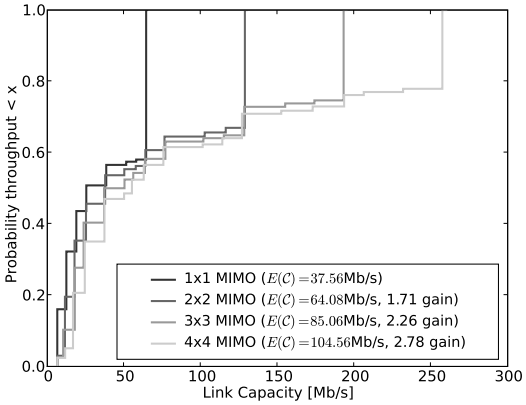

(a) IMT-A UMi BSS

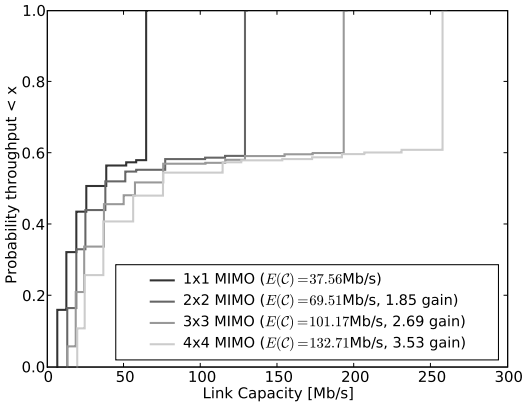

(b) IMT-A UMi BSS without MIMO antenna correlation

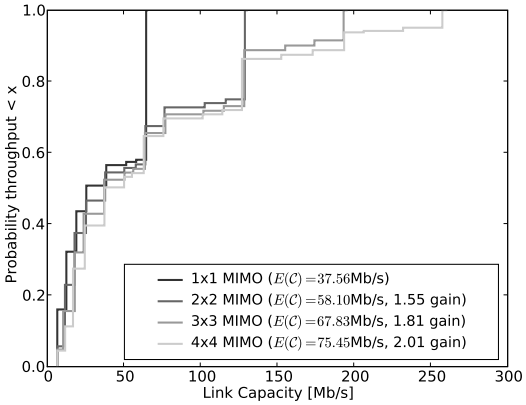

(c) IMT-A UMi BSS with high MIMO antenna correlation

Fig. 3: CDF of the capacity in a BSS.

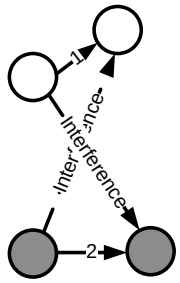

Fig. 4: Example network to demonstrate the effect of concurrent transmissions.

the network potentially doubles the number of possible combinations of active links, making the capacity calculation hard for any larger network.

A. Capacity Limits

The system model considers the restrictions and opportunities a node is constrained by and able to exploit, respectively. To find the capacity of the WMN, we apply an optimal scheduler that is able to plan concurrent transmissions optimally.

Time is assumed to be divided into fixed scheduling intervals of duration I. During one interval, a node i generates a load of l_{ij} directed to node j. This is expressed by the traffic requirement T which defines source, destination and the load. For example, the traffic requirement

$$T = \left\{ \begin{array}{ccc} \text{(source)} & \text{(rate)} & \text{(destination)} \\ N_2 & \rightarrow^{1\,\text{Mb}} & N_1 \\ N_6 & \rightarrow^{1\,\text{Mb}} & N_1 \\ N_1 & \rightarrow^{1\,\text{Mb}} & N_7) \end{array} \right\}.$$

specifies in three rows the loads from N_2 to N_1, N_6 to N_1 and N_1 to N_7, with 1 Mb each.

The task of the scheduler is to generate the sequence of transmissions such that this load is transported. This sequence is represented as the *schedule* $\big((\mathrm{S}_1, \delta_1)\,; (\mathrm{S}_2, \delta_2)\,; \ldots ; \big(\mathrm{S}_{|\mathcal{S}|}, \delta_{|\mathcal{S}|}\big)\big)$ of network states S_i and durations δ_i, with $0 \leq \delta_i \leq 1$ and $\mathcal{S}$ the set that contains all network states.

Each *network state* represents a possible combination of active links, given by transmitter, receiver, rate, source and destination of the packet flow. An example state would be

$$\mathrm{S} = \left\{ \begin{array}{ccccc} \text{(source)} & \text{(tx)} & \text{(rate)} & \text{(rx)} & \text{(destination)} \\ (N_2 \rightsquigarrow) & N_2 & \rightarrow^{54\,\text{Mb/s}} & N_3 & (\rightsquigarrow N_1) \\ (N_6 \rightsquigarrow) & N_5 & \rightarrow^{12\,\text{Mb/s}} & N_4 & (\rightsquigarrow N_1) \\ (N_1 \rightsquigarrow) & N_1 & \rightarrow^{24\,\text{Mb/s}} & N_7 & (\rightsquigarrow N_7) \end{array} \right\}.$$

This example specifies in three rows three simultaneous transmissions, one from node N_2 to node N_3 at 54 Mb/s with data originated at node N_2 and addressed to

node N_1; another from N_5 to N_4 at 12 Mb/s originated from node N_6 and addressed to N_1, etc.

A network state is *feasible* if each transmission contained is possible according to the system model. A feasible schedule must contain feasible network states only; furthermore, it must fulfil the offered traffic requirements such that if S_i is active for δ_i, $1 \leq i \leq |\mathcal{S}|$, the requirements from T are met.

The sum $\sum_{i=1\ldots|\mathcal{S}|} \delta_i$ gives the duration of the complete schedule. If this duration is larger than the duration of the scheduling interval I, more traffic is generated than what can be transported by the schedule. A schedule is called optimal if no other feasible schedule exists that has a smaller duration; let δ_i^* denote the corresponding optimal duration for network state S_i. Then the minimum resource utilisation to carry the traffic given in T using the network states $\mathcal{S}$ is

$$\mathrm{RU}(\mathcal{S}, T) = \sum_{i=1\ldots|\mathcal{S}|} \delta_i^*. \tag{20}$$

As defined in [10], the *capacity region* $\mathcal{C}(\mathcal{S})$ of a WMN with network states $\mathcal{S}$ is the set of all load settings T for which a feasible schedule exists:

$$\mathcal{C}(\mathcal{S}) = \{T : \mathrm{RU}\,(\mathcal{S}, T) \leq I\}\,. \tag{21}$$

The convex hull of $\mathcal{C}(\mathcal{S})$, i. e., the set of all T where $\mathrm{RU}\,(\mathcal{S}, T) = I$, describes the capacity limits of the WMN under any possible partitioning of resources among the (source-destination)-pairs in the network.

Therefore, the dimension of the capacity region is the number of STAs, n_{STA}, in the WMN, as each can have a different load. To reduce the number of dimensions, we compute only the *uniform system capacity* $\mathcal{C}^u(\mathcal{S})$, defined as the point of the capacity where all n_{STA} STAs have the same load l:

$$\mathcal{C}^u(\mathcal{S}) = \frac{n_{STA} \cdot l}{\mathrm{RU}\,(\mathcal{S}, T)}. \tag{22}$$

The calculation of the optimal schedule is performed $\mathcal{C}^u(\mathcal{S})$ in two steps: In step one, the set $\mathcal{S}$ of all feasible network states is computed. The second step converts T and each network state into a matrix such that the optimisation problem of finding the optimal schedule becomes an instance of Linear Programming (LP):

$$\begin{aligned} &\text{minimise } f(\delta) = \sum_{i=1\ldots|\mathcal{S}|} \delta_i \\ &\text{such that } \sum_{i=1\ldots|\mathcal{S}|} \delta_i \cdot \mathbf{s}_i = T \\ &\qquad 0 \leq \delta_i \leq 1 \qquad i = 1 \ldots |\mathcal{S}|. \end{aligned} \tag{23}$$

The complexity of both parts of the algorithm, namely the creation of the network states and the solving of the LP instance, depends on the number of network states $\mathcal{S}$ to be considered. As shown in [10], this number is expected to increase exponentially with the number of nodes, which limits the applicability to networks having less than 30 nodes.

[13] proposes heuristics to optimise the generation of the network states such that the upper bound capacity is closely approximated. Thereby, up to 150 nodes become feasible.

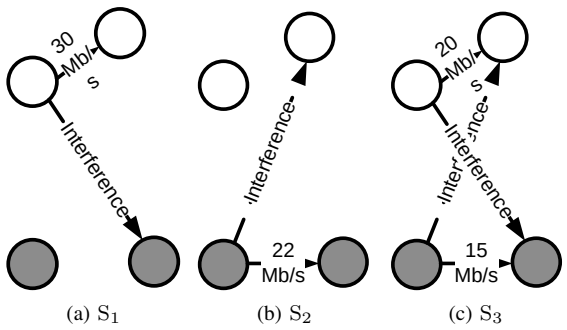

(a) S_1 (b) S_2 (c) S_3

Fig. 5: The network states of the network in Figure 4.

B. Example

The example network in Figure 4 is used to illustrate network states and the resulting capacity region.

The network has two links and three network states, depicted in Figure 5: link 1 active, link 2 active, or both links active. In this network, the computation of the capacity region $\mathcal{C}(\mathcal{S})$ given in Figure 6 is simple owing to the small number of network states:

- The intersections with the x- and y-axis are given by schedules where only S_1 respectively S_2 is active.
- The throughput of a schedule where only S_3 is active cannot be achieved by any linear combination of S_1 and S_2; hence, the point $(20/15)$ is part of the hull.
- The remaining hull is a linear combination of either S_1 with S_3 if link 1 needs to transmit more than 20 Mb (and link 2 less than 15 Mb), or S_2 with S_3 in the opposite case. Any combination of S_1 and S_2 would result in lower throughput for one of the links.

The uniform system capacity $\mathcal{C}^u(\mathcal{S})$ can be found by restricting T to the points where the load of link 1 is equal to link 2. The capacity limit under this condition is given by $T = (440/27, 440/27)$, resulting in $\mathcal{C}^u(\mathcal{S}) \approx 32.6$ Mb/s.

VI. Evaluation

For the evaluation, we apply the WMN scenario creator from [27]. It is used to generate 10 scenarios of 1 km^2 each with different shadowing conditions; then, each scenario is covered with around 20 MSTAs with AP functionality so that wireless coverage and connectivity of the WMN is ensured.

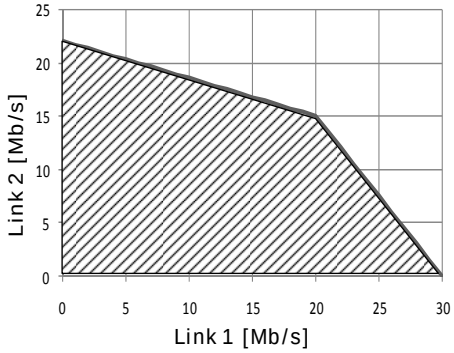

Fig. 6: Capacity region of the network in Figure 4.

In the second step, either all, 6, 4 or 2 of the MSTAs equipped with mesh gate functions, i. e., connected to the wired backbone; this results in approximately 0, 2.5, 5 or 10 MSTAs per mesh gate, respectively. Then, costs for every link in the WMN are calculated by the maximum transmission rate on the link; this allows for creating a routing matrix using the Dijkstra all-pairs shortest path matrix.

Traffic is generated in each scenario by 100 STAs, positioned randomly and associated to the closest (in terms of pathloss) AP. Each STA requests downlink and uplink traffic from/to the Internet, divided as 90 to 10. Downlink traffic origins at the mesh gate closest to the STA (in terms of path cost), uplink traffic is destined to this mesh gate. By combining the randomly generated offered traffic and the routing matrix, a traffic requirement for each link in the network can be calculated, composing the load matrix T[1].

Then, the capacity calculation procedure as described above is applied in each scenario, resulting in a scenario-specific value for $\mathcal{C}^u$. Dividing this capacity by the number of MSTAs results in the mean BSS capacity of the scenario; this value allows for comparison to the values found in the single BSS case, Section IV. Finally, the scenario-specific mean BSS capacity is averaged over the 10 different scenarios, resulting in an estimation for the expected BSS capacity in a WMN. Besides this expected BSS capacity, we calculate and plot the confidence interval for a 95% confidence level of the mean capacity estimator.

Similar to Figure 3, three different settings for the MIMO model are considered: First, the default UMi values as given in Table I. Then, for comparison, the antenna correlation is minimised by setting the angle spread of the MSTAs and STAs to π. Finally, the

[1]Optionally, T can only contain the end-to-end loads and the optimal routes through the WMN are found automatically during the schedule minimisation. However, a STA might be associated to multiple APs and distribute its traffic over multiple routes, then. As routing is not the scope of this work, the routes are pre-calculated as described.

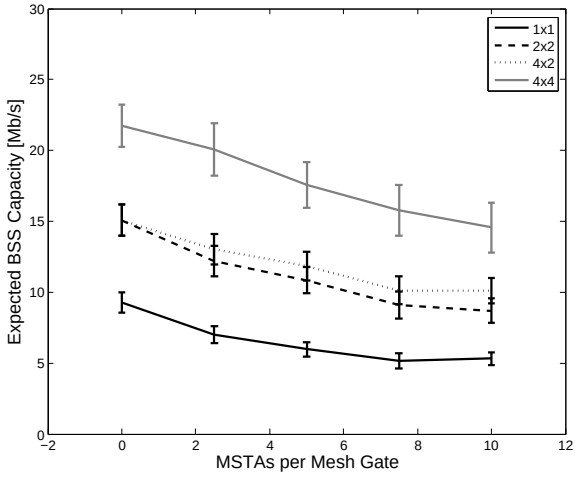

(a) UMi MIMO settings.

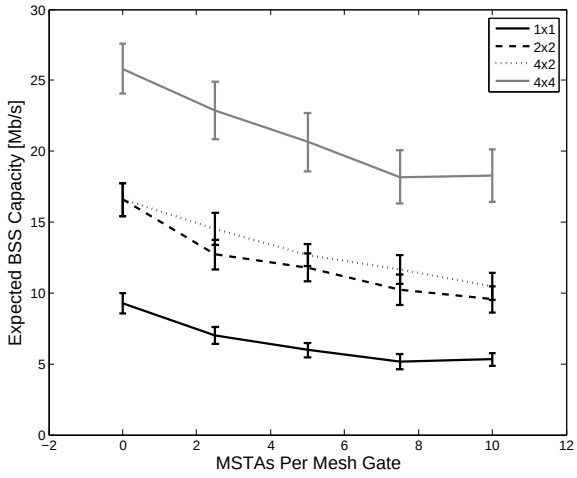

(b) No MIMO antenna correlation.

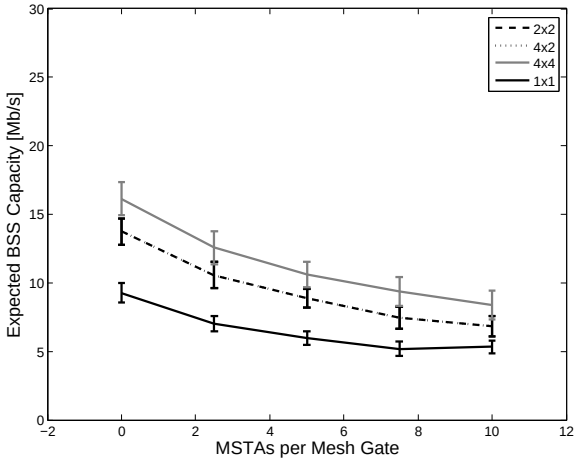

(c) High MIMO antenna correlation.

Fig. 7: Expected BSS capacity of the WMN. In axb, a is for the number of antennas of MSTAs, b for STAs

angle spread values from the IMT-A SMa are used to demonstrate a scenario setting with high correlation and low MIMO performance.

The baseline antenna configuration is a "traditional" Single Input/Single Output (SISO) equipment: All devices – MSTAs and STAs – only have a single antenna. Of course, the BSS capacity for the baseline configuration is independent of the MIMO model parameter settings, as they only impact the performance in the multi-antenna case. Nevertheless, the results from the baseline configuration are given in all figures for comparison.

The other MIMO configurations assume either 2 or 4 antennas at all devices; Additionally, a "4x2" case is given where all MSTAs are configured with 4 antennas, whereas the STAs have 2 antennas only.

Figure 7 presents the expected BSS capacity for the different MIMO configurations and model parameter settings.

Clearly, the interference from the neighbouring BSSs reduces the BSS capacity significantly below the expected capacity of a single BSS given in Figure 3. In case of a network without MSTAs, i. e., a traditional multi-AP deployment, the BSS capacity decreases by a factor of four. Interestingly, this decrease is independent of the antenna configuration and the MIMO model setting. Consequently, the capacity increase of MIMO in the single BSS is completely translated into a capacity increase in the multi BSS network, i. e., the same non-linear increase as found in Section IV is also present. For example, using the UMi MIMO model parameters, the expected capacity increases compared to the 1x1 case by a factor of 1.6 and 2.4 for the 2x2 and 4x4 configuration, respectively.

As expected, the introduction of MSTAs reduces BSS capacity. The more MSTAs per mesh gateway are deployed, the higher the mean number of hops in the WMN, which cannot be countered completely by an increase of concurrent transmissions. However, the theoretical link capacity gain of MIMO is better approached by the higher the number of MSTAs.

For the 5 MSTAs per mesh gate deployment and the UMi MIMO model setting, the expected capacity increase factors are 1.9 (2x2) and 2.9 (4x4) when compared to the 1x1 case. Without antenna correlation, these factors become 2.0 and 3.5, respectively.

The reason for a higher MIMO gain in the WMN deployment is found in the capacity distribution of links in the backbone of the WMN: According to the node placement algorithm from [27], "good" positions for MSTAs are preferred, leading to a high SINR between adjacent MSTAs in the WMN. Hence, a 1x1 link is improved more than what can be expected from the average improvement as calculated in Section IV. This improvement of few links is visible in the final results because the capacity of the WMN backbone limits the capacity of the whole WMN; hence, an improvement of few, but important links leads to an improvement of the complete network capacity.

VII. Conclusion

Both WMN and MIMO are interesting research fields on their own. In this paper, we show that the combination of both gains valuable insights: WMNs benefit significantly from the capacity increase of MIMO.

The results, based on the capacity calculation framework, represent upper bound capacities. It is not clear what remains of this capacity if a real MAC protocol, using an imperfect (distributed) scheduler, is applied: Introducing MIMO to WMNs increases the chance of the rate adaptation algorithms to apply different MCSs; consequently, more errors can be made by the scheduler, resulting in uncoordinated concurrent transmissions. Consequently, distributed scheduling of MIMO-enhanced WMNs appears to be a promising research area.

Acknowledgements

The work leading to these results has been partly funded by the European Community's Seventh Framework Program FP7/2007-2013 under grant agreement no. 213311 also referred as OMEGA project.

References

[1] S. Max and T. Wang, "Transmit power control in wireless mesh networks considered harmful," in *Second International Conference on Advances in Mesh Networks, 2009 (MESH 2009)*, (Athens, Greece), pp. 73–78, Jun 2009.

[2] IEEE, "IEEE 802.11n-2009: Standard for Information technology - Telecommunications and information exchange between systems - Local and Metropolitan Area Networks - Specific Requirements - Part 11: Wireless LAN Medium Access Control (MAC) & Physical Layer specifications - Enhancements for Higher Throughput," Amedment 802.11n, New York, Sept. 2009.

[3] IEEE, "IEEE 802.11s/D5.0: Draft Standard for Information technology - Telecommunications and information exchange between systems - Local and Metropolitan Area Networks - Specific Requirements - Part 11: Wireless LAN Medium Access Control (MAC) & Physical Layer specifications - Amendment 10: Mesh Networking," Amedment 802.11s, New York, Apr. 2010.

[4] P. Gupta and P. R. Kumar, "The capacity of wireless networks," *IEEE Transactions on Information Theory*, vol. 46, no. 2, pp. 388–404, 2000.

[5] B. Liu, Z. Liu, and D. Towsley, "On the capacity of hybrid wireless networks," in *Proc. of the IEEE Conference on Computer Communications (INFOCOM)*, Mar. 2003.

[6] M. Grossglauser and D. N. C. Tse, "Mobility increases the capacity of ad-hoc wireless networks," in *Proc. of the IEEE Conference on Computer Communications (INFOCOM)*, pp. 1360–1369, Apr. 2001.

[7] K. Jain, J. Padhye, V. N. Padmanabhan, and L. Qiu, "Impact of interference on multi-hop wireless network performance," *Wireless Netwoks*, vol. 11, pp. 471–487, July 2005.

[8] V. S. A. Kumar, M. V. Marathe, S. Parthasarathy, and A. Srinivasan, "Algorithmic aspects of capacity in wireless networks," in *Proc. of the ACM SIGMETRICS Conference*, (Banff, Canada), pp. 133–144, June 2005.

[9] E. Arikan, "Some complexity results about packet radio networks," *IEEE Transactions on Information Theory*, vol. 30, pp. 681–685, July 1984.

[10] S. Toumpis and A. J. Goldsmith, "Capacity regions for wireless ad hoc networks," *IEEE Transactions on Wireless Communications*, vol. 2, pp. 736–748, July 2003.

[11] P. Bjorklund, P. Varbrand, and D. Yuan, "Resource optimization of spatial tdma in ad hoc radio networks: a column generation approach," in *INFOCOM 2003. Twenty-Second Annual Joint Conference of the IEEE Computer and Communications. IEEE Societies*, vol. 2, pp. 818–824 vol.2, March-3 April 2003.

[12] S. Max, G. R. Hiertz, E. Weiss, D. Denteneer, and B. H. Walke, "Spectrum sharing in ieee 802.11s wireless mesh networks," *Computer Networks*, vol. 51, pp. 2353–2367, June 2007.

[13] S. Max, E. Weiss, G. Hiertz, and B. Walke, "Capacity bounds of deployment concepts for wireless mesh networks," *Performance Evaluation*, vol. 66, pp. 272–286, Mar 2009.

[14] S. Max, L. Stibor, G. Hiertz, and D. Denteneer, "On the performance of hybrid wireless/wired mesh networks," in *Proceedings of the 3rd IEEE International Conference on Wireless and Mobile Computing, Networking and Communications WiMob 2007*, (White Plains, New York, USA), p. 8, IEEE Computer Society, Oct 2007.

[15] S. Max, E. Weiss, and G. Hiertz, "Analysis of wimedia-based uwb mesh networks," in *In Proceedings of the 32nd IEEE Conference on Local Computer Networks (LCN) 2007*, (Dublin, Ireland), pp. 919–926, IEEE Computer Society, Oct 2007.

[16] ITU, "Rep. ITU-R M.2135, Guidelines for evaluation of radio interface technologies for IMT-Advanced," report, ITU, 2008.

[17] J. G. Proakis, *Digital Communications*. Mcgraw-Hill Publ.Comp., 4. a. ed., Aug. 2000.

[18] M. Pursley and D. Taipale, "Error probabilities for Spread-Spectrum packet radio with convolutional codes and viterbi decoding," *Communications, IEEE Transactions on*, vol. 35, no. 1, pp. 1–12, 1987.

[19] J. Mirkovic, G. Orfanos, and H. Reumerman, "MIMO link modeling for system level simulations," in *Personal, Indoor and Mobile Radio Communications, 2006 IEEE 17th International Symposium on*, pp. 1–6, 2006.

[20] D. Gesbert, M. Shafi, D. shan Shiu, P. Smith, and A. Naguib, "From theory to practice: an overview of MIMO space-time coded wireless systems," *Selected Areas in Communications, IEEE Journal on*, vol. 21, no. 3, pp. 281–302, 2003.

[21] J. Heath, R.W. and A. Paulraj, "Linear dispersion codes for mimo systems based on frame theory," *Signal Processing, IEEE Transactions on*, vol. 50, pp. 2429 – 2441, oct 2002.

[22] H. Bölcskei, M. Borgmann, and A. J. Paulraj, "Impact of the propagation environment on the performance of space-frequency coded MIMO-OFDM," *IEEE Journal on Selected Areas in Communications*, vol. 21, pp. 427–439, Apr. 2003. Final version 2002-11-30.

[23] D. Asztely, "On Antenna Arrays in Mobile Communication Systems," Tech. Rep. IR–S3–SB–9611, Royal Institute of Technology, Department of Signals, Sensors & Systems, Stockholm, 1996.

[24] X. Li and Z. Nie, "Effect of array orientation on performance of MIMO wireless channels," *Antennas and Wireless Propagation Letters, IEEE*, vol. 3, pp. 368–371, 2004.

[25] D. Gore, R. Heath, and A. Paulraj, "On performance of the zero forcing receiver in presence of transmit correlation," in *Information Theory, 2002. Proceedings. 2002 IEEE International Symposium on*, p. 159, 2002.

[26] M. McKay and I. Collings, "Error performance of MIMO-BICM with Zero-Forcing receivers in Spatially-Correlated rayleigh channels," *Wireless Communications, IEEE Transactions on*, vol. 6, no. 3, pp. 787–792, 2007.

[27] S. Max, L. Stibor, G. Hiertz, and D. Denteneer, "IEEE 802.11s mesh network deployment concepts -invited paper-," in *Proc. of European Wireless Conference 2007*, (Paris, France), Apr. 2007.